Effect of an Intersubunit Disulfide Bond on the Stability of *Streptomyces* Subtilisin Inhibitor†

Atsuo Tamura,‡ Shuichi Kojima,§ Kin-ichiro Miura,§ and Julian M. Sturtevant*,‡

Department of Chemistry, Yale University, New Haven, Connecticut 06520, and Institute of Biomolecular Science, Gakushuin University, Mejiro, Tokyo 171, Japan

Received April 26, 1994; Revised Manuscript Received September 16, 1994⊗

ABSTRACT: The effect of an engineered disulfide bond between two identical subunits of a dimeric protein, *Streptomyces* subtilisin inhibitor, on the stability of the protein was studied by differential scanning calorimetry. The introduction of the linkage caused a large stabilization without changing the cooperativity of unfolding, with the denaturation temperature of a 2 mg/mL solution being increased by 14.3 °C to 95.0 °C at pH 9.5 and by 16.4 °C to 63.0 °C at pH 3.0. The stabilization was caused by a loss of denaturational entropy, i.e., −40 and −98 cal K^{-1} mol^{-1} at pH 3.0 and 9.5, respectively, which more than compensated for the loss in the denaturational enthalpy.

The role of disulfide bonds in the stabilization of proteins is a somewhat controversial topic. It was presumed that the effect of disulfide bonds on the stability was mainly due to a decrease in the conformational chain entropy of the unfolded polypeptide chain (Flory, 1956). In the case of ribonuclease T1, Pace et al. (1988) correlated the change in conformational entropy of the unfolded form with the number of amino acid residues between the side chains that are cross-linked and demonstrated the applicability of this correlation to several other proteins. The addition of newly introduced disulfide bonds by protein engineering, however, did not always confer an increase in stability (Matsumura & Matthews, 1991), mainly due to the strain introduced into the native structure. In general, the introduction of covalent linkages into proteins has caused either stabilizing or destabilizing effects, which are caused not only by entropic factors but also by enthalpic factors, as reviewed by Sturtevant (1994).

To date, all of these experiments have been performed with intramolecular cross-links, except for the introduction of an intersubunit disulfide bond in λ repressor (Sauer et al., 1986), with the stability being examined by spectroscopic methods such as CD and NMR. Although the spectroscopic measurements give us van't Hoff enthalpies, the true (calorimetric) enthalpy and related thermodynamic parameters can only be obtained from calorimetric measurements. Recently, the effect of an intersubunit disulfide linkage on the stability of the Cro repressor of phage λ was examined in detail by differential scanning calorimetry (DSC) (Gitelson et al., 1991; Griko et al., 1992) and showed not only the stabilization effect but also other complexities, such as a change in the size of the cooperative unit in unfolding.

In the present work, we have successfully introduced an intersubunit disulfide bond into a dimeric protein, *Streptomyces* subtilisin inhibitor (SSI). In contrast to the case of the Cro repressor of phage λ, the denaturation of this protein followed a two-state scheme, as for the wild type, resulting in the evaluation of the calorimetric enthalpy and other thermodynamic parameters for the linkage. The parameters thus obtained should help to explain the effect of an intersubunit disulfide bond on stability.

It is known that SSI exists as a homodimer in the native state and dissociates to monomers in the heat (or cold) denatured state, as shown in the following scheme (eq 1) (Takahashi & Sturtevant, 1981; Tamura et al., 1991b,c). The addition of an intersubunit linkage will change the denaturation to a nondissociative form in the denatured protein, as shown in eq 2:

$$N_2 \rightleftharpoons 2D \quad (1)$$

$$N \rightleftharpoons D \quad (2)$$

where N in eq 2 is structurally identical to N_2 in eq 1, except for the introduced disulfide linkage.

The amino acid residues selected for replacement with Cys were Val13, Thr32, and Asp83, which are geometrically close enough to form intersubunit disulfide bonds. Among these mutations, only Asp83 replaced by Cys (designated as D83C) could be obtained as a purified protein sample, while the other two mutants presented difficulties in expression, presumably because of folding problems. As a control, a mutant whose Asp83 is replaced by Asn (designated as D83N) was also prepared. By this modest replacement, the effect of the loss of the negative charge at position 83 could be taken into account.

Although the mutation did not change the cooperative unit, it did change the intermolecular interaction between D molecules at pH values below 2.0, resulting in the appearance of an extra peak in the DSC curve at higher temperatures. This phenomenon will be analyzed using an appropriate curve-fitting program.

MATERIALS AND METHODS

Mutagenesis of the Asp83 Codon of the SSI Gene. Codon substitution of Asp83 (GAC) to Asn (AAC) or Cys (TGC)

† This research was supported in part by Grant GM-04725 from the National Institutes of Health, Grant MCB-9120192 from the National Science Foundation, and the Toyobo Science Foundation.

* Author to whom correspondence should be addressed.

‡ Yale University.

§ Gakushuin University.

⊗ Abstract published in *Advance ACS Abstracts,* November 1, 1994.

0006-2960/94/0433-14512$04.50/0

was carried out by site-directed mutagenesis, followed by cassette mutagenesis of a plasmid pSIAX that contains the *Aat*II−*Xba*I fragment of the coding region of the SSI gene. Initially, the *Fsp*I site was generated at the position of Trp86 in the pSIAX by site-directed mutagenesis (Morinaga et al., 1984) using a mutagenic primer, 5′-AC-GGC-GTT*-G*C*G-CAG-GGC-3′, where the asterisks indicate the mismatched bases. The mutated plasmid was designated as pSIAX-*Fsp*I. For cassette mutagenesis, oligodeoxynucleotides 5′-C-ATG-TGC-CCG-ATG-GTG-TAC-G-3′ (fragment I), 5′-GG-GTC-GTA-CAC-CAT-CGG-GCA-CAT-GAC-GT-3′ (fragment II), 5′-AC-CCG-GTG-CTG-CTG-ACC-GTG-XXX-GGC-GTC-TG-3′ (fragment III; XXX is AAC for Asn83 and TGC for Cys83), and 5′-CA-GAC-GCC-XXX-CAC-GGT-GAG-CAG-CAC-C-3′ (fragment IV; XXX is GTT for Asn83 and GCA for Cys83) were synthesized. After phosphorylation at the 5′-termini, fragments I and II and fragments III and IV were annealed, respectively. These two fragments were further annealed to produce a 51 bp fragments. Since pSIAX-*Fsp*I has two *Fsp*I sites, pSIAX-*Fsp*I was digested with *Fsp*I and *Bgl*I, and 1500 bp of the *Fsp*I−*Bgl*I fragment were isolated. On the other hand, pUC18 was digested with *Aat*II and *Bgl*I, and 800 bp of the *Aat*II−*Bgl*I fragment were isolated. The annealed synthetic fragment and the two isolated fragments were ligated and transferred into *Escherichia coli* JM109. The mutated plasmid was identified by colony hybridization using fragment IV as a probe, and mutation was confirmed by dideoxy sequencing. Reconstruction of mutated pSI52 from the mutated pSIAX, insertion of the SSI gene into *Streptomyces* plasmid pIJ702, and transformation of *Streptomyces lividans* 66 were carried out as described previously (Kojima et al., 1990).

Purification of Protein. Purification of the protein sample was carried out following the same procedure as that previously reported (Tamura et al., 1991a). The wild-type SSI, as well as the mutant SSIs in this paper, was prepared from a strain of *Streptomyces lividans* 66 transformed by the SSI gene without mutation. The difference between this SSI and that from the original strain, *Streptomyces albogriseolus* S-3253, however, is just three extra amino acid residues in the N-terminus (Obata et al., 1989). A molecular weight of 23 000 as a dimer (Hiromi et al., 1985) was used for all the mutants, since the changes in the molecular weight caused by the mutations are negligible.

Determination of Inhibitor Constant. A synthetic substrate, *N*-succinyl-L-Ala-LAla-L-Pro-L-Phe-*p* nitroanilide (sAAPF-pNA), was used for determination of the inhibitor constant (K_i) of mutated SSI toward subtilisin BPN′. The procedure was described in a previous paper (Kojima et al., 1990).

DSC Measurements. SSI samples were dialyzed overnight against two changes of a 25 mM Gly buffer at either acidic or alkaline pH or a 25 mM phosphate buffer at neutral pH. The concentration of the protein solution after dialysis was determined spectroscopically, using the absorption at 280 nm for a 1 mg/mL solution of 0.796 (Hiromi et al., 1985). The pH values shown later are those of the dialysate. Calorimetric measurements were made with MC-2 (Microcal, Inc., Northampton, MA) and DASM-4 (Biopribor, Puschino, Russia) calorimeters, which gave closely agreeing results. A scan rate of 1 K min^{-1} was employed throughout. The instrumental baseline, which was recorded prior to scanning each sample with both cells filled with dialysate, was subtracted from the sample scan, in which the sample cell was filled with protein solution. In some cases, especially when the pH was close to the isoelectric point of SSI (p*I* = 4.3) and the protein was subject to aggregation, the cell assembly of the MC-2 calorimeter was rotated 90 deg in order to reduce convective disturbances of the intercell thermopile. It has been found empirically that such disturbances are decreased or completely eliminated when the vertical dimension of the cell is reduced from about 1 cm to approximately 1 mm. We have no explanation for this phenomenon.

Data Analysis. Data analysis was carried out according to the procedure reported earlier (Sturtevant, 1987) with a modified program using the Marquardt method for nonlinear least-squares fitting (Marquardt, 1963). The model, which is a modified two-state model for both cases 1 and 2, has three viable parameters, i.e., Δh_{cal}, the calorimetric enthalpy in calories per gram, $t_{1/2}$, the temperature at which the reaction is half-complete, and β, which is equal to $\Delta H_{vH}/\Delta h_{cal}$. In this paper, capital letters denote values per mole and small letters denote those per gram. The details of the program for the analysis of the reaction with self-association and dissociation will be shown in the Appendix.

RESULTS

The formation of an intersubunit disulfide bond was confirmed by SDS−PAGE (sodium dodecyl sulfate−polyacrylamide gel electrophoresis), with and without a reducing reagent. The lanes of the wild type and D83C in the presence of β-mercaptoethanol showed similar mobility, whereas those without β-mercaptoethanol showed significantly slower movement for D83C. The difference in mobility of D83C in the nonreducing conditions indicated the formation of an intersubunit disulfide bond. On the other hand, D83C in 8 M guanidium chloride solution did not react with DTNB (5,5′-dithiobis(2-nitrobenzoic acid)), indicating that no free SH group existed, namely, the intersubunit disulfide bond between the two Cys83 residues in each subunit was formed completely.

Inhibitor constants for D83C and D83N were obtained as $(1.9 \pm 0.2) \times 10^{-11}$ and $(2.5 \pm 0.3) \times 10^{-11}$ mol L^{-1}, respectively, showing strong binding to subtilisin BPN′. Comparison with the inhibitor constant of the wild-type protein (5×10^{-12} mol L^{-1}; Kojima et al., 1990) indicates that these mutations, which are far from the reactive site and buried inside the protein, caused little effect on the binding to subtilisin BPN′.

Figure 1 shows typical DSC scans of the wild-type SSI and D83C at various pH's. In the case of the wild-type SSI at acidic pH, linearity for the native state can only be obtained at pH values above 2.9 due to the emergence of cold denaturation at lower pH values (Figure 1A at pH 2.59). At pH values above 3.3, aggregation occurred after the denaturation due to the closeness to the isoelectric point, resulting in an aberration of the DSC curve (Takahashi & Sturtevant, 1981). In the case of D83C, the scans could be extended to lower pH values (down to 2.3) because of the lack of cold denaturation. At pH values lower than 2.3, however, the emergence of an intermolecular interaction, which will be mentioned later, prevented us from analyzing the data using the program for the simple two-state model. At pH values above 3.3, the same problem as in the case of the wild type arose due to aggregation.

The stabilities of the wild type and D83N change very little between pH 7.00 and 9.75. Because of the fact that

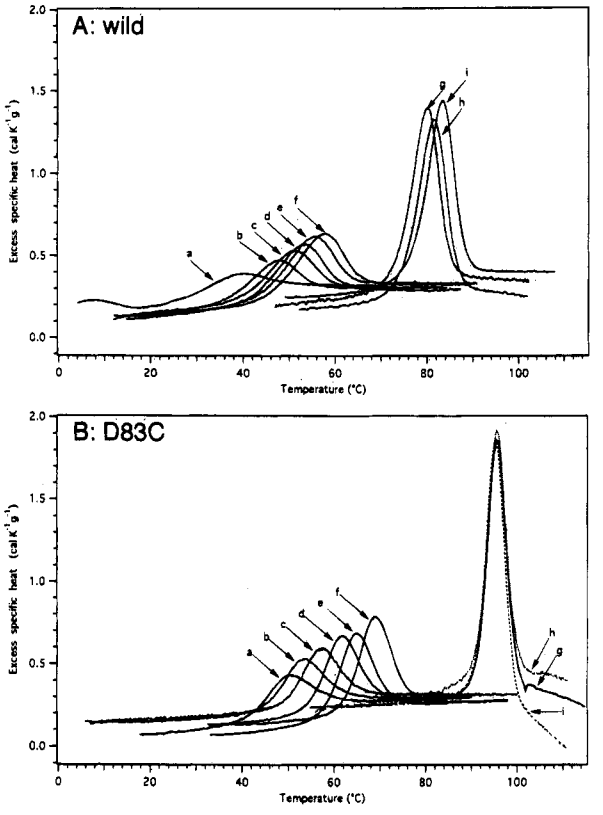

FIGURE 1: DSC curves for solutions at various pH's with the wild-type SSI (A) and D83C (B). All of the curves shown here were measured on the MC-2 calorimeter. The pH values and concentrations of the protein are as follows: (A) a, pH 2.59, 4.52 mg mL^{-1}; b, pH 2.94, 2.40 mg mL^{-1}; c, pH 3.07, 2.16 mg mL^{-1}; d, pH 3.15, 2.17 mg mL^{-1}; e, pH 3.21, 2.11 mg mL^{-1}; f, pH 3.25, 2.26 mg mL^{-1}; g, pH 9.20, 1.13 mg mL^{-1}; h, pH 9.50, 2.15 mg mL^{-1}; i, pH 7.00, 2.50 mg mL^{-1}. (B) a, pH 2.37, 2.38 mg mL^{-1}; b, pH 2.50, 2.21 mg mL^{-1}; c, pH 2.68, 2.33 mg mL^{-1}; d, pH 2.94, 2.25 mg mL^{-1}; e, pH 3.07, 2.44 mg mL^{-1}; f, pH 3.25, 2.25 mg mL^{-1}; g, pH 7.00, 2.53 mg mL^{-1}; h, pH 7.00, 1.20 mg mL^{-1}; i, pH 9.50, 2.46 mg mL^{-1}.

the concentration dependence of the stability has disappeared in the case of the monomeric protein D83C, all of these peaks shown in Figure 1B for solutions at neutral pH with different protein concentrations and at alkaline pH are almost coincidental. When the pH value exceeded 9.2, the apparent specific heat of the denatured state of the wild type decreased linearly, with a steeper slope at higher pH, preventing us from getting analyzable results at pH values above 9.8. In the case of D83C at neutral pH or above, with the denaturation temperature exceeding 95 °C, the posttransition baseline usually had a negative slope and became too steep to analyze at pH values above 9.5. All possible measurements were carried out, taking into account the restrictions mentioned earlier.

Figure 2 shows typical results of curve fitting for the wild-type SSI (pH 3.15) and D83C (pH 2.68). The wild type fits well to the model of the dissociative two-state scheme (eq 1) and D83C fits to the nondissociative scheme (eq 2). All of the results obtained in 34 experiments with the wild type, 28 experiments with D83C, and 16 experiments with D83N are summarized in Table 1.

DISCUSSION

The reversibility of denaturation was examined by scanning the temperature up to the point of 95% completion of denaturation, followed by immediate cooling and rescanning. Typically, those two scans showed full reproducibility. There were two exceptions in the case of D83C. One is at neutral pH or higher, at which the temperature of 95% completion is over 100 °C, and the other is at pH values below 2.0, where intermolecular interaction emerged upon denaturation, as will be mentioned later. In both cases, reversibility was 70−85%.

The average values of $\Delta H_{vH}/\Delta H_{cal}$ are 1.01 (±0.05), 1.01 (±0.06), and 0.995 (±0.046) for the wild-type, D83C, and D83N, respectively. The ratio $\Delta H_{vH}/\Delta H_{cal}$ is close to unity, showing that the denaturations are well represented by the two-state model in all cases. The ratio is close to or exceeds 1.1 for D83C at neutral pH or higher, suggesting that some type of intermolecular association, presumably in the denatured state, is present in these cases. The average of the ratio $\Delta H_{vH}/\Delta H_{cal}$ in the acidic pH region for D83C is 0.983 (±0.033).

The calorimetric enthalpy obtained experimentally includes not only the heat of the conformational transition of the protein but also those of the ionization of both the protein and the buffer (Privalov, 1979):

$$\Delta h_{cal} = \Delta h_{conf} + \Delta h_{ion\ pr} + \Delta h_{ion\ buf} \qquad (3)$$

where Δh_{conf} is the enthalpy for the conformational transition of the protein, $\Delta h_{ion\ pr}$ is that for the ionization of the protein, and $\Delta h_{ion\ buf}$ is that for the ionization of the buffer. In acidic or alkaline solution, the heat of ionization upon denaturation of a carboxyl or amino group within the protein is approximately compensated by that of the glycine buffer. The heat of ionization of His, however, cannot be compensated, resulting in an additional heat. SSI has two histidines: one, His106, with a pK_a value of 6.4 as determined by ^1H NMR in ^2H_2O at 25 °C, and the other, His43, which is not titratable in the native form and can only be protonated in the denatured form (HIromi et al., 1985; Tamura et al., 1991a). Thus, the heat of protonation of His43 upon denaturation contributes to the enthalpy experimentally obtained in the acidic pH range, while in the alkaline pH range it does not because its charge remains unchanged. The calorimetric enthalpy for the protonation of histidine is −7.14 kcal mol^{-1} at 25 °C (Izatt & Christensen, 1970) and that of glycine is 0.98 kcal mol^{-1} at 25 °C and 0.47 kcal mol^{-1} at 40 °C. Since the heat capacity change typically is small for the protonation of an imidazole group (H. Fukada & K. Takahashi, personal communication), we used the value at 25 °C of −7.14 kcal mol^{-1}, or −0.621 cal g^{-1}, in the case of SSI as the heat of protonation throughout. On the other hand, if the negative heat capacity change holds, the heat of protonation of glycine is supposed to be close to zero at the denaturation temperature of SSI (around 50 °C). Thus, no correction was made for the ionization of the buffer. The conformational enthalpies thus calculated by correcting for the heat of protonation of histidine at acidic pH are listed in the fourth column of Table 1. Since little or no protonation of His 43 occurs at neutral or higher pH, Δh_{cal} is assumed to be the same as Δh_{conf} in this region. Other candidates for the contribution of heat of ionization are Tyr residues. In the case of SSI, however, pK_a's of Tyr7, Tyr75, and Tyr93 are 11.0, 11.8, and 12.6, respectively, indicating that they do not affect the enthalpy in these experiments, which were carried out at pH values below 9.8.

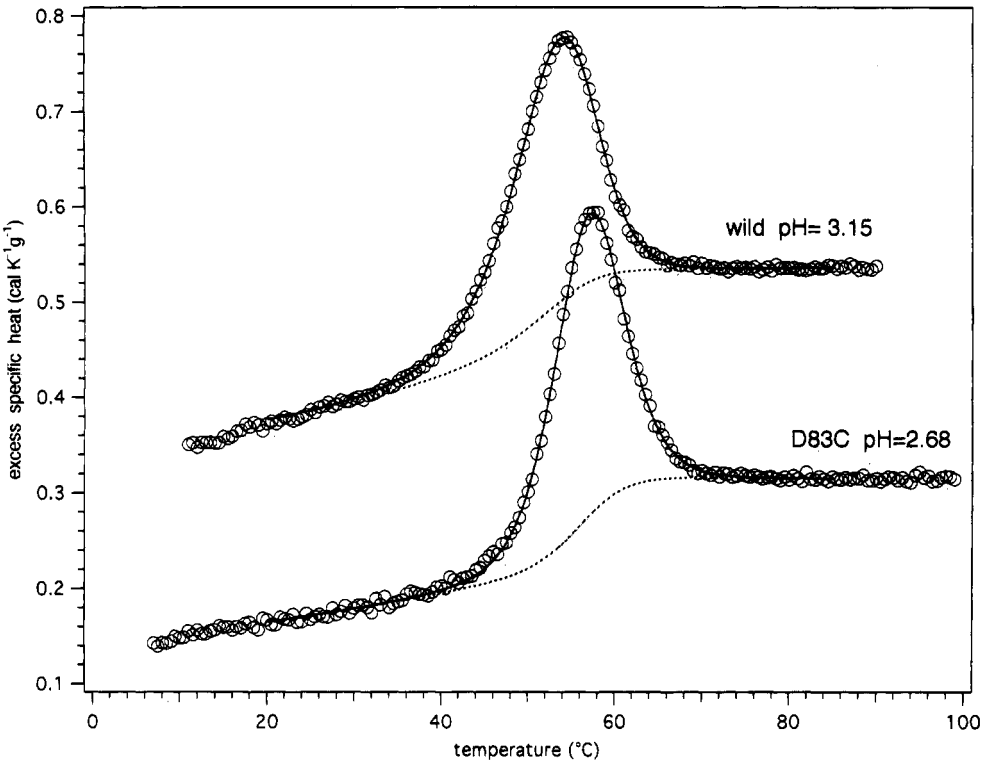

FIGURE 2: Tracings of typical DSC curves for the wild-type SSI at pH 3.15 and 2.06 mg mL^{-1} and for D83C at pH 2.68 and 2.33 mg mL^{-1}. The curve for the wild-type SSI was shifted upward for display purposes: observed data (O); the number of points being reduced by half, calculated curve (—) and calculated base line (- - -).

The plots of Δh_{conf} against $t_{1/2}$ in Figure 3 show excellent linearity over the entire temperature region. The expressions for Δh_{conf} obtained by linear least squaring are as follows:

$$\text{wild type:}\quad \Delta h_{conf} = -2.149\ (\pm 0.105) + 0.1268\ (\pm 0.0017)t$$

$$\text{D83C:}\quad \Delta h_{conf} = -1.528\ (\pm 0.123) + 0.1006\ (\pm 0.0018)t$$

$$\text{D83N:}\quad \Delta h_{conf} = -1.995\ (\pm 0.111) + 0.1271\ (\pm 0.0018)t \quad (4)$$

The uncertainties indicated are the standard errors of the respective constants. It is to be noted that the slopes for the wild type and D83N are close, while D83C has a smaller slope.

The slopes in eqs 4 can be regarded as values for ΔC_p. In some cases, the values for ΔC_p obtained as shown here are found to be in reasonable agreement with the mean values obtained from individual DSC scans (Hu et al., 1992a; Ladbury et al., 1992), but in other cases this is not found to be true (Hu et al., 1992b). With the present proteins there are also significant differences: the average values for ΔC_p obtained from the individual scans are 0.0892 (±0.0218) for the wild-type protein, 0.0851 (±0.0210) for D83C, and 0.0888 (±0.0186) for D83N, all of which are smaller than the corresponding slopes in eqs 4. In view of the intrinsic uncertainties in the ΔC_p values from the individual scans, hereafter we employ the slopes in eqs 4 as the specific heat changes in the unfolding of these proteins.

The smaller ΔC_p for D83C compared to that for the wild type presumably is due to less exposure of the hydrophobic amino acid residues in the denatured structure. Δh_{conf} for D83C is significantly lower than that of the wild type, suggesting that enthalpic attractions such as van der Waals interactions and hydrogen bonding existing in the native structure are not completely destroyed in the denatured structure.

Thermodynamic parameters, represented by the molar quantities ΔH, $\Delta S°$, and $\Delta G°$, are calculated as follows:

$$\Delta H(T) = \Delta H(T_{1/2}) + \Delta C_p(T - T_{1/2}) \quad (5)$$

$$\Delta S°(T) = \Delta S°(T_{1/2}) + \Delta C_p \ln(T/T_{1/2}) \quad (6)$$

where ΔC_p is also the quantity per mole. At $T_{1/2}$, where the extent of conversion is 0.5, $\Delta G°$ is

$$\Delta G°(T_{1/2}) = \Delta H(T_{1/2}) - T_{1/2}\Delta S°(T_{1/2})$$

Therefore, $\Delta G°(T)$ is expressed as

$$\Delta G°(T) = \Delta H(T_{1/2}) - (T/T_{1/2})(\Delta H(T_{1/2}) - \Delta G°(T_{1/2})) + \Delta C_p(T - T_{1/2} - T\ln(T/T_{1/2})) \quad (7)$$

The term $\Delta G°(T_{1/2})$ in eq 8, which is zero in the case of eq 2, can be expressed using the equilibrium constant K and the total concentration c in the case of eq 1:

$$\Delta G°(T_{1/2}) = -RT_{1/2} \ln K(T_{1/2}) = -RT_{1/2} \ln(2c) \quad (8)$$

Molar free energy changes upon thermal unfolding of the wild-type SSI, D83C, and D83N at pH 9.5 and 3.0, as a function of temperature and calculated on the basis of eq 7, are shown in Figure 4. The curve for D83C is shallower than the others because of the smaller ΔC_p. Since the free energy for the scheme in eq 1 has the additional term in eq 7, the curves for the wild type and D83N are generally

Table 1: Thermodynamic Parameters for the Thermal Unfolding of Wild-Type SSI and Its D83C and D83N Mutant Forms

pH	concn (mg mL^{-1})	$t_{1/2}$ (°C)	Δh_{conf} (cal g^{-1})	$\Delta H_{vH}/\Delta H_{cal}$	ΔC_p (cal g^{-1} K^{-1})	SD (% of C_{max})	pH	concn (mg mL^{-1})	$t_{1/2}$ (°C)	Δh_{conf} (cal g^{-1})	$\Delta H_{vH}/\Delta H_{cal}$	ΔC_p (cal g^{-1} K^{-1})	SD (% of C_{max})
							Wild Type						
2.90	2.17	44.45	3.56	1.05	0.120	1.6	3.21	2.11	53.09	4.65	0.951	0.0981	1.1
2.94	2.40	43.93	3.45	1.07	0.121	0.7		2.22	53.67	4.59	1.00	0.0845	1.2
2.98	2.26	45.35	3.64	1.09	0.0951	1.2	3.24	2.19	54.30	4.84	0.909	0.103	1.1
3.03	2.21	47.78	4.04	1.02	0.0901	1.6	3.25	2.26	55.64	4.87	0.948	0.0768	1.4
3.04	1.16	44.41	3.57	1.09	0.135	1.5		2.39	55.73	4.83	0.917	0.0935	0.6
	2.27	47.61	3.88	1.05	0.114	0.8	7.00	0.531	80.65	8.05	0.996	0.0728	1.3
	4.54	50.11	4.12	0.906	0.123	1.4		1.10	81.56	8.11	1.01	0.0645	0.5
	2.21	48.34	4.01	1.04	0.0907	1.1		2.26	82.21	8.27	1.03	0.0670	0.2
3.07	2.26	48.52	4.04	1.01	0.107	2.6		2.45	82.46	8.26	0.986	0.0860	0.4
	2.16	49.02	4.03	1.08	0.0807	1.1		4.06	83.23	8.49	1.01	0.0532	0.3
3.12	2.16	49.64	4.23	1.04	0.0787	1.1	9.20	1.13	79.22	7.98	1.02	0.0772	0.3
	2.46	51.38	4.23	0.985	0.0980	0.5		2.26	80.51	8.07	1.02	0.0383	0.4
3.15	2.06	51.42	4.33	0.980	0.100	0.7		2.27	80.16	8.02	1.01	0.0666	0.2
	2.17	51.10	4.33	1.05	0.0753	1.1		3.02	80.55	8.22	1.00	0.0782	0.1
3.16	2.52	51.51	4.33	0.942	0.134	0.9	9.50	2.15	80.70	8.08	0.990	0.0776	0.3
	2.07	52.84	4.51	1.00	0.0930	1.5	9.75	2.16	80.22	7.96	1.02	0.0896	0.2
3.19	2.32	53.34	4.50	0.969	0.0730	0.9	mean ± SD				1.01 ± 0.05	0.0892 ± 0.0218	
3.20	2.36	53.62	4.59	0.992	0.0799	0.9							
							D83C						
2.30	2.03	47.95	3.31	0.978	0.0966	2.2	3.04	2.21	63.22	4.93	0.946	0.0852	0.4
2.37	2.38	48.94	3.39	0.971	0.100	1.7	3.07	2.44	64.48	5.02	0.956	0.0712	0.5
2.40	2.27	49.95	3.59	0.981	0.0842	2.1	3.15	1.99	66.63	5.07	0.966	0.0795	0.5
2.50	2.21	52.51	3.75	1.00	0.0824	1.1	3.16	2.42	66.48	5.22	0.933	0.0781	0.4
2.56	2.34	53.16	3.79	1.02	0.0999	1.1	3.25	2.25	68.72	5.47	0.936	0.0625	0.4
2.59	2.05	54.30	3.94	1.03	0.0743	1.1		2.40	68.90	5.27	0.958	0.0753	0.4
	2.33	54.08	3.88	1.02	0.0871	1.0	7.00	0.605	95.37	7.97	1.09	0.0345	0.9
2.68	2.33	56.20	4.02	1.01	0.0988	0.9		1.20	95.30	8.09	1.07	0.0772	1.0
2.79	2.25	58.91	4.28	1.00	0.0780	0.6		2.53	95.30	7.98	1.11	0.0958	0.9
2.80	1.98	58.84	4.35	1.03	0.0844	0.8	9.50	0.617	94.99	8.17	1.08	0.129	1.5
2.88	1.18	59.66	4.40	1.03	0.0463	1.1		1.24	94.95	7.97	1.12	0.131	1.3
	2.23	59.89	4.51	0.993	0.0922	0.5		2.46	94.97	8.07	1.10	0.112	1.4
	4.70	60.05	4.54	0.921	0.0994	0.5	9.75	2.47	94.82	2.08	1.11	0.0573	1.3
2.89	2.04	60.51	4.64	0.996	0.0889	0.7	mean ± SD				1.01 ± 0.06	0.0851 ± 0.0210	
2.94	2.25	61.18	4.72	0.971	0.0801	0.6							
							D83N						
2.90	2.25	42.28	3.33	1.06	0.101	2.0	3.20	2.22	51.32	4.60	0.936	0.0997	1.3
2.94	2.35	44.81	3.62	1.08	0.0949	1.7	3.21	2.29	51.31	4.55	0.934	0.117	1.2
2.98	2.20	45.15	3.83	1.04	0.0497	2.9	7.00	0.588	82.27	8.47	0.943	0.0717	0.8
3.00	2.16	45.73	3.92	1.03	0.0753	0.9		1.18	83.10	8.57	0.997	0.0838	0.3
3.04	2.33	46.33	3.89	1.01	0.106	1.5		2.35	83.90	8.62	0.996	0.790	0.2
3.07	2.24	47.34	3.98	1.03	0.0981	1.5	95.0	2.17	82.58	8.57	0.986	0.0692	1.1
3.15	2.24	50.23	4.35	0.990	0.0925	1.1	9.75	1.84	82.28	8.41	1.00	0.0785	0.3
3.16	2.28	49.90	4.28	0.951	0.115	1.0	mean ± SD				0.995 ± 0.046	0.0888 ± 0.0186	
3.19	2.45	51.39	4.55	0.931	0.0803	0.7							

positioned high. However, it is to be noted that $t_{1/2}$ values for the wild type and D83N are the crossing point of the free energy curves with the line $-RT \ln K(T_{1/2})$, whereas $t_{1/2}$ for D83C is where the free energy is zero.

Thermodynamic parameters ΔH, $\Delta S°$, and $\Delta G°$, evaluated at $t_{1/2}$ for the wild-type SSI at pH 3.0, 3.2, 7.0, and 9.5 (obtained using eqs 5−7), are summarized in Table 2. The gain in stability due to the disulfide bridge is caused entirely by the entropic factor, which more than compensates for the decrease in the enthalpic term. One source of this loss in entropy is the cratic entropy (Kauzmann, 1959), −8.0 cal K^{-1} (mol·dimer)$^{-1}$, arising from the loss of translational entropy due to the intermolecular cross-link. However, the differences in the entropy of unfolding, $\Delta\Delta S°$, which are −40, −51, −99, and −98 cal K^{-1} mol^{-1} at pH 3.0, 3.2, 7.0, and 9.5, respectively, are far larger than the cratic entropy. Therefore, the large loss in the denaturational entropy, which results in the large stabilizations, i.e., $t_{1/2}$ increased by 16.4 °C at pH 3.0 or by 14.3 °C at pH 9.5, was mainly caused by other factors. Less exposure of hydrophobic residues reflected by the smaller ΔC_p should cause higher ΔS because of less ordering of solvents (hydrophobic effect), which is in opposition to the experimentally observed entropy loss. Therefore, the main source for this loss of entropy comes from the configurational entropy of structuring the peptide chains and side chains in the denatured structure, which overcomes the hydrophobic effect. Structurally, it is likely that the linkage between the two subunits caused the formation of a residual structure in the interface of the subunits.

Figure 5A shows the plots of $t_{1/2}$ against pH in the acidic region for the solutions with D83C and for those with the wild type and D83N in the concentration range of protein around 2.2 mg/mL. They are well represented as linear functions:

$$\text{wild type:}\quad t_{1/2} = -55.06\ (\pm 8.42) + 33.88\ (\pm 2.70)\text{pH}$$

$$\text{D83C:}\quad t_{1/2} = -2.36\ (\pm 1.65) + 21.78\ (\pm 0.58)\text{pH}$$

$$\text{D83N:}\quad t_{1/2} = -39.02\ (\pm 7.64) + 28.22\ (\pm 2.48)\text{pH} \qquad (9)$$

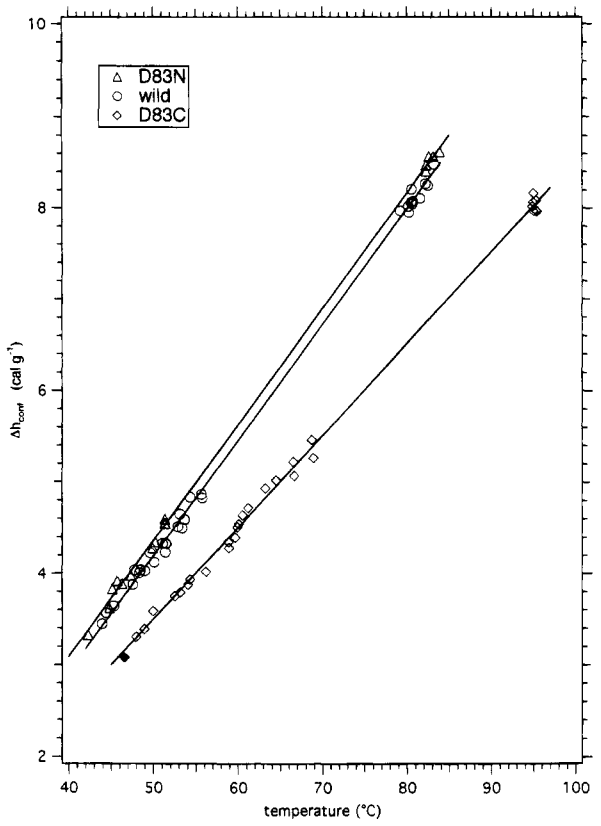

FIGURE 3: Conformational enthalpy change of thermal denaturation of the wild-type SSI (○), D83C (◇), and D83N (△) plotted as a function of $t_{1/2}$, the temperature of half-completion of the denaturation. The lines shown in the figure are $-2.149 + 0.1268t$ for the wild type, $-1.528 + 0.1006t$ for D83C, and $-1.995 + 0.1271t$ for D83N, which were obtained by least-squares fitting. The point, ◆, shows the plot of Δh_{h1} after exclusion of the heat of His43 protonation against t_{h1} obtained from the analysis for D83C at pH 1.65, which was excluded from the least-squares fitting.

The slopes in eq 9, in conjunction with the following equation derived from the van't Hoff equation

$$\Delta\nu = \frac{1000\Delta H_{cal}}{2.303RT_{1/2}^2}\frac{dt_{1/2}}{dpH} \qquad (10)$$

where $\Delta\nu$ is the number of protons taken up from the buffer during denaturation, lead to the following results:

$$\text{wild type:}\quad \Delta\nu = -10.63\ (\pm1.56) + 5.30\ (\pm0.50)\text{pH}$$

$$\text{D83C:}\quad \Delta\nu = -1.05\ (\pm0.29) + 1.70\ (\pm0.10)\text{pH}$$

$$\text{D83N:}\quad \Delta\nu = -8.20\ (\pm1.94) + 4.21\ (\pm0.63)\text{pH} \qquad (11)$$

over the acidic pH range covered here, as shown in Figure 5B. The difference between the wild type and D83N is due to the loss of a carboxyl group induced by the replacement of Asp83 with Asn. On the other hand, the difference between D83N and D83C shows that the loss of Asp83 is not the only reason for the difference in the denaturational change in the protonation in the case of D83C.

D83C showed unusual behavior at pH values below 2.0. Figure 6 shows the DSC scans of D83C at pH 1.65 at different protein concentrations. The DSC curves showed

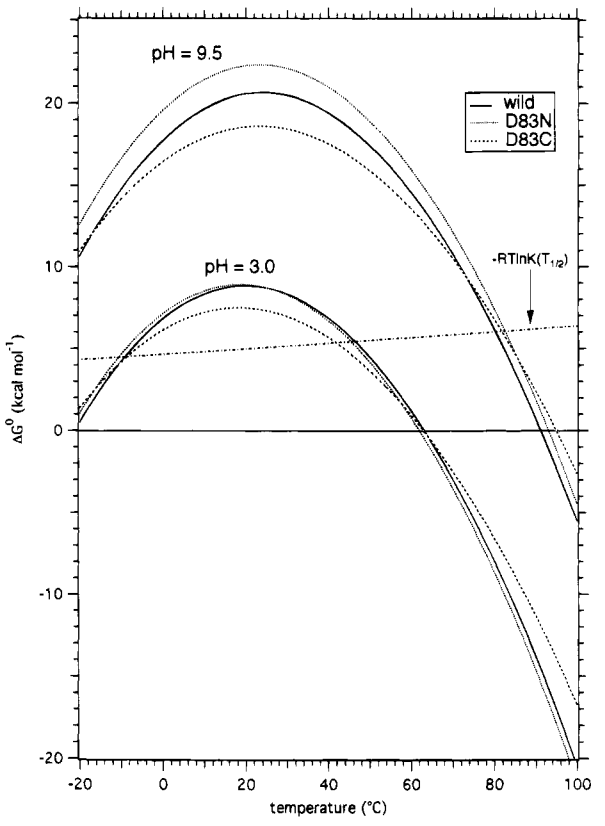

FIGURE 4: Molar free energy changes upon thermal unfolding of wild-type SSI (—), D83C (- - -), and D83N (···) at pH 3.0 and 9.5 as a function of temperature, calculated on the basis of eq 8.

Table 2: Thermodynamic Parameters for Denaturation at $t_{1/2}$ of the Wild-Type SSI

	wild-type SSI	D83C	D83N
ΔC_p (cal g^{-1} K^{-1})	0.1268 (±0.0017)	0.1006 (±0.0018)	0.1271 (±0.0018)
	pH 3.0		
concn (mg mL^{-1})	2.25	(2.23)[a]	2.28
$t_{1/2}$ (°C)	46.58	62.98	45.64
$\Delta G°$ (kcal mol^{-1})	5.432	4.464	5.168
ΔH (kcal mol^{-1})	86.42	72.63	90.28
$\Delta S°$ (cal K^{-1} mol^{-1})	253.3	213.2	266.2
	pH 3.2		
concn (mg mL^{-1})	2.25	(2.23)[a]	2.28
$t_{1/2}$ (°C)	53.36	67.34	51.28
$\Delta G°$ (kcal mol^{-1})	5.549	4.276	4.866
ΔH (kcal mol^{-1})	106.2	88.32	110.1
$\Delta S°$ (cal K^{-1} mol^{-1})	308.3	257.4	322.3
	pH 7.0		
concn (mg mL^{-1})	2.26	(2.53)[a]	2.35
$t_{1/2}$ (°C)	82.21	95.30	83.90
$\Delta G°$ (kcal mol^{-1})	6.034	6.062	6.912
ΔH (kcal mol^{-1})	190.3	155.1	194.4
$\Delta S°$ (cal K^{-1} mol^{-1})	518.6	419.4	527.6
	pH 9.5		
concn (mg mL^{-1})	2.15	(2.46)[a]	2.17
$t_{1/2}$ (°C)	80.70	94.97	82.58
$\Delta G°$ (kcal mol^{-1})	6.044	6.522	7.024
ΔH (kcal mol^{-1})	185.9	151.6	190.0
$\Delta S°$ (cal K^{-1} mol^{-1})	508.4	410.0	517.1

[a] Concentrations of D83C are unnecessary for the calculation of thermodynamic parameters.

two peaks: the peak temperature of the first one becomes lower at higher concentrations, whereas that of the second peak became higher, suggesting the existence of some type of associated structure(s) in the range between the two peaks.

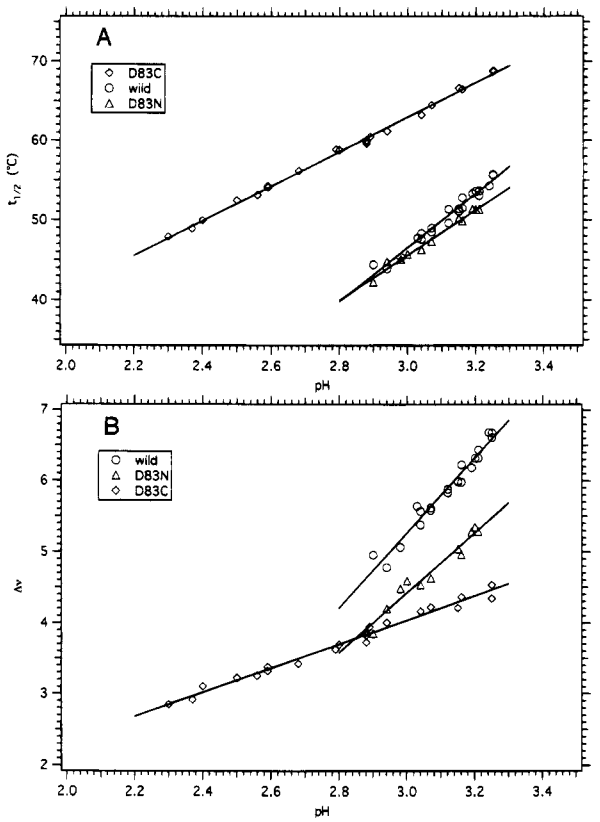

FIGURE 5: (A) Variation with pH of the temperature of half-completion of denaturation, $t_{1/2}$, for wild-type protein (○), D83C (◇), and D83N (△). Included in the figure are the least-squared lines for the wild type, −55.06 + 33.88pH, for D83C, −2.36 + 21.78pH, and for the D83N, −39.02 + 28.22pH. (B) Variation with pH of the denaturational increase in the number of protons bound by the proteins, $\Delta\nu$, for the wild-type (○), D83C (◇), and D83N (△). Included in the figure are the least-squared lines for the wild type, −10.63 + 5.298pH, for D83C, −1.051 + 1.697pH, and for D83N, −8.201 + 4.208pH.

By using the simplest associated form, i.e., a dimer, the reaction can be represented by the scheme

$$N \rightleftharpoons D \rightleftharpoons {}^1/_2D_2 \qquad (12)$$

The first reaction is the denaturation, with positive enthalpy Δh_1, and the second reaction is the intermolecular association, with negative enthalpy Δh_2. In order for the reaction to proceed by increasing the temperature, $\Delta h_1 + \Delta h_2$ must be positive. This means that the denaturation proceeded, coupled with some extent of dimerization depending on the equilibrium constants, and then eventually the dissociation was completed by increasing the temperature. Note that all of the dimeric molecules are formed after passing through the denaturation. Thus, the first peak corresponds to the reaction N → D (denaturation) and second to $^1/_2D_2$ → D (dissociation).

The result of the curve-fitting (see the Appendix) to the data for a 2.15 mg mL^{-1} solution at pH 1.65 and the change in the population of each species calculated from the parameters obtained from the fitting are shown in Figure 7A,B, respectively. As Figure 7 shows, the denaturation occurred at first coupled with some extent of dimerization depending on the equilibrium constant between the monomer and the dimer, consisting of the first peak. Following this is the dissociation of the dimer, and eventually all of the molecules turned into the monomeric denatured structure, consisting of the second peak. The beginning of the peak

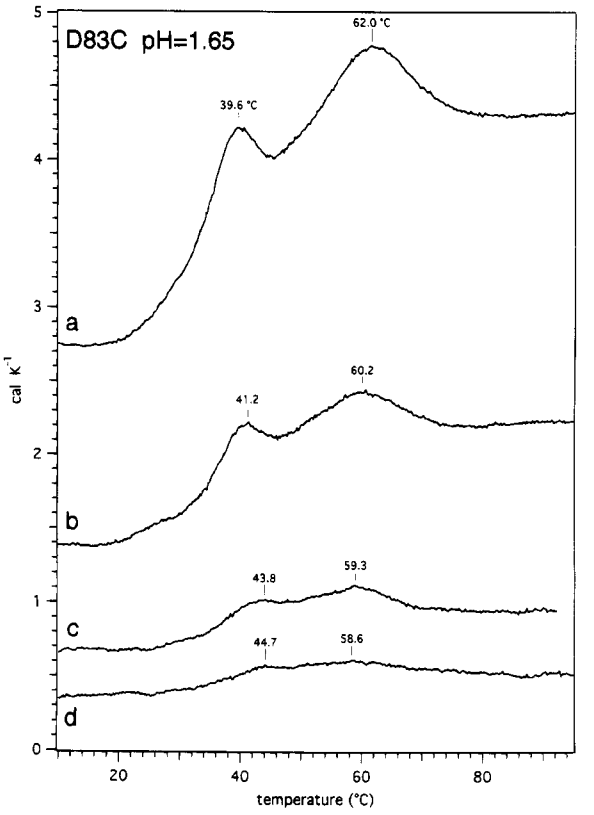

FIGURE 6: Concentration dependence of the DSC curves for D83C at pH 1.65: (a) 8.46 mg mL^{-1}; (b) 4.17 mg mL^{-1}; (c) 2.15 mg mL^{-1}; (d) 1.09 mg mL^{-1}. The numbers indicated in the DSC curves are the peak temperatures evaluated graphically.

starting at around 0 °C is the cold denaturation between N and D. Note that no dimerization is expected to occur at low temperatures. At concentrations higher than 2.15 mg mL^{-1}, the curve-fitting was not successful due to the extremely large apparent ΔC_p, suggesting the existence of other reactions involving such molecules as highly aggregated forms. The parameters obtained as a result of curve-fitting at 2.15 mg mL^{-1} are Δh_{h1} = 2.46 cal/g, Δh_{h2} = 1.50 cal/g, β_1 = 23 900, β_2 = 16 900, t_{h1} = 46.61 °C, t_{h2} = 53.65 °C, and ΔC_p at t_{h1} between N and D was 0.0768 cal g^{-1} K^{-1}. The plot of Δh_{h1} after exclusion of the heat of His43 protonation against t_{h1} is located close to the line of the plot of Δh_{conf} against $t_{1/2}$ in the two-state denaturation model, as shown in Figure 3, supporting the validity of the scheme in eq 12.

ACKNOWLEDGMENT

We are indebted to Dr. Y. Takeuchi for the use of computer graphics in designing the disulfide linkage, to Dr. K. Akasaka and K. Kimura for the purification of protein samples, and to Dr. J. Thomson for helpful discussions.

APPENDIX

This curve-fitting program is intended for a reaction with two consecutive reactions, one being denaturation and the other dimerization of the denatured structure, both with a change in C_p. The reaction is represented in the scheme in eq 12:

$$\begin{array}{ccccc} & \overset{\Delta h_1}{\underset{K_1}{\rightleftharpoons}} & & \overset{\Delta h_2}{\underset{K_2}{\rightleftharpoons}} & \\ N & & D & & {}^1/_2D_2 \\ c(1-\alpha_1-\alpha_2) & & c\,\alpha_1 & & {}^1/_2c\,\alpha_2 \quad \text{(mol/L)} \end{array}$$

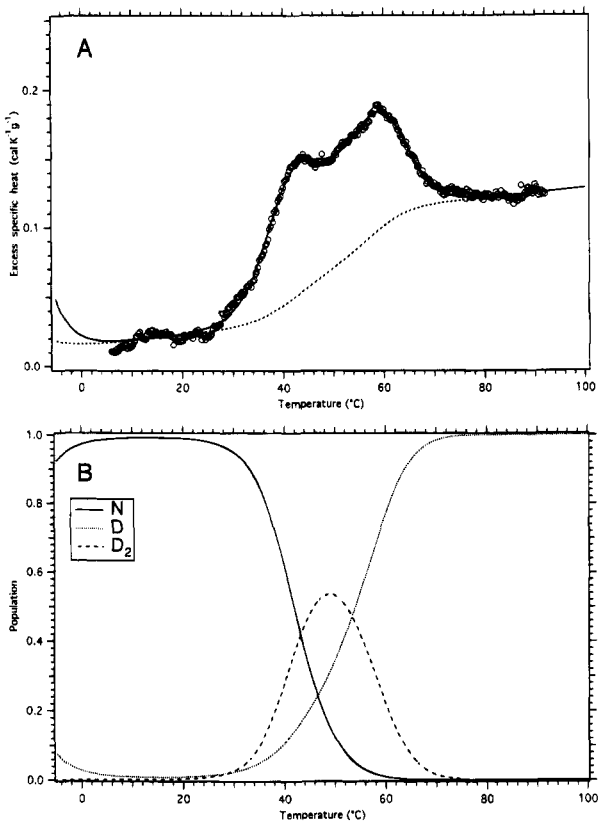

FIGURE 7: (A) Tracings of the DSC curve of a 2.15 mg mL^{-1} solution of D83C at pH 1.65: observed data (○), calculated curve (—), and calculated baseline (- - -) based on the curve-fitting procedure described in the Appendix. The parameters obtained as a result of curve fitting are $\Delta h_{h1} = 2.46$ cal g^{-1}, $\Delta h_{h2} = -1.50$ cal g^{-1}, $\beta_1 = 23\,900$, $\beta_2 = 16\,900$, $t_{h1} = 46.61$ °C, $t_{h2} = 53.65$ °C, and ΔC_p between N and D at t_{h1} was 0.0768 cal g^{-1} K^{-1}. (B) Temperature dependence of the populations of N, D, and D_2 corresponding to the curve-fitting shown in A.

where Δh_1, the heat of denaturation is positive, and Δh_2, the heat of dimerization, is negative, and as indicated in Discussion, $\Delta h_1 + \Delta h_2$ is positive. K_1 and K_2 are the equilibrium constants for each reaction, α_1 and α_2 are the extent of conversion from N to D and from N to D_2, respectively, and c is the total molar concentration.

The equilibrium constants are

$$K_1 = \frac{[D]}{[N]} = \frac{\alpha_1}{1 - \alpha_1 - \alpha_2} \quad \text{(A1)}$$

$$K_2 = \frac{[D_2]^{1/2}}{[D]} = \frac{1}{\sqrt{2c}} \frac{\sqrt{\alpha_2}}{\alpha_1} \quad \text{(A2)}$$

so that

$$\alpha_1 = \frac{2K_1}{1 + K_1 + \sqrt{(1 + K_1)^2 + 8cK_1^2K_2^2}} \quad \text{(A3)}$$

$$\alpha_2 = 2cK_2^2\alpha_1^2 \quad \text{(A4)}$$

The apparent specific heat of the native protein, C_N, that of the denatured protein, C_N, that of the denatured protein, C_D, and that of the dimerized denatured protein, C_{D_2}, are assumed to be linear functions of the temperature:

$$C_N + A_1 + A_2t, \quad C_D = C_1 + C_2t, \quad C_{D2} = B_1 + B_2t \quad \text{(A5)}$$

where A_1, A_2, B_1, B_2, C_1, and C_2 are constants and t is the temperature in °C. A_1, A_2, C_1, and C_2 are evaluated by linear least squaring of pre- and posttransition baselines. Since it is usually impossible to observe the baseline for the intermediate state, C_{D_2} is assumed to be proportional to the heats of the reactions:

$$C_{D_2} = C_N + \frac{\Delta h_{cal1} + \Delta h_{cal2}}{\Delta h_{cal1}}(C_D - C_N) \quad \text{(A6)}$$

The specific enthalpies for the reactions N → D (Δh_{cal1}) and D → D_2 (Δh_{cal2}) are then

$$\Delta h_{cal1} = \Delta h_{01} + (C_1 - A_1)t + {}^1/_2(C_2 - A_2)t^2 \quad \text{(A7)}$$

$$\Delta h_{cal2} = \Delta h_{02} + (B_1 - C_1)t + {}^1/_2(B_2 - C_2)t^2 \quad \text{(A8)}$$

where

$$\Delta h_{01} = \Delta h_{h1} - (C_1 - A_1)t_{h1} - {}^1/_2(C_2 - A_2){t_{h1}}^2 \quad \text{(A9)}$$

$$\Delta h_{02} = \Delta h_{h2} - (B_1 - C_1)t_{h2} - {}^1/_2(B_2 - C_2){t_{h2}}^2 \quad \text{(A10)}$$

with t_{h1} and t_{h2} being the temperatures of half-completion and Δh_{h1} and Δh_{h2} being the enthalpies at t_{h1} and t_{h2}, respectively.

From the van't Hoff equation, the temperature dependencies of the equilibrium constants are expressed as follows:

$$R/\beta_1 \ln\left(\frac{K_1(T)}{K_1(T_{h1})}\right) = AA_1\left(\frac{1}{T} - \frac{1}{T_{h1}}\right) + BB_1 \ln(T/T_{h1}) + CC_1(T - T_{h1}) \quad \text{(A11)}$$

$$R/\beta_2 \ln\left(\frac{K_2(T)}{K_2(T_{h2})}\right) = AA_2\left(\frac{1}{T} - \frac{1}{T_{h2}}\right) + BB_2 \ln(T/T_{h2}) + CC_2(T - T_{h2}) \quad \text{(A12)}$$

where

$$T = 273.15 + t$$

$$AA_1 \equiv -\Delta h_{01} + 273.15(C_1 - A_1) - {}^1/_2(273.15)^2(C_2 - A_2)$$

$$BB_1 \equiv (C_1 - A_1) - 273.15(C_2 - A_2)$$

$$CC_1 \equiv {}^1/_2(C_2 - A_2)$$

$$AA_2 \equiv -\Delta h_{02} + 273.15(B_1 - C_1) - {}^1/_2(273.15)^2(B_2 - C_2)$$

$$BB_2 \equiv (B_1 - C_1) - 273.15(B_2 - C_2)$$

$$CC_2 \equiv {}^1/_2(B_2 - C_2)$$

$K_1(T_{h1})$ and $K_2(T_{h2})$ can be calculated by putting $\alpha_1 = 0.5$ or $\alpha_2 = 0.5$ in eqs A1 and A2, respectively:

$$K_1(T_{h1}) = \frac{1}{1 - cK_2^2(T_{h1})} \quad \text{(A13)}$$

$$K_2(T_{h2}) = \left(1 + \frac{1}{K_1(T_{h2})}\right)/\sqrt{c} \qquad \text{(A14)}$$

Equations A13 and A14 must be incorporated into the curve-fitting in conjunction with eqs A11 and A12. The initial value of $K_1(T_{h1})$ is set to 1, or that of $K_2(T_{h2})$ is set to $1/(c)^{1/2}$ in the program. In this case, half-completion means the point where the mole fraction of one species is equal to the total of the other two. However, the definitions of T_{h1} and T_{h2} are arbitrary, since half-completion can also be defined as the point where the mole fractions between two molecular species in either one of the reactions are the same. In the latter definition, T_{h1} and T_{h2} are the temperatures at which K_1 and K_2 are 1 and $1/(c)^{1/2}$, respectively. These two methods are legitimate as long as the definition is clear. Therefore, in this paper, we employed the latter definition for simplicity.

In order to calculate the excess specific heat, it is necessary to obtain not only the expression of α_1 and α_2 but also the derivatives of α_1 and α_2. From the van't Hoff equation and eqs A1 and A2

$$\frac{\beta_1 \Delta h_{cal1}}{RT^2} = \frac{d \ln K_1}{dT} = \frac{1}{\alpha_1}\frac{d\alpha_1}{dT} + \frac{1}{1-\alpha_1-\alpha_2}\left(\frac{d\alpha_1}{dT} + \frac{d\alpha_2}{dT}\right) \qquad \text{(A15)}$$

$$\frac{\beta_2 \Delta h_{cal2}}{RT^2} = \frac{d \ln K_2}{dT} = -\frac{1}{\alpha_1}\frac{d\alpha_1}{dT} + \frac{1}{2\alpha_2}\frac{d\alpha_2}{dT} \qquad \text{(A16)}$$

Then the derivatives for α_1 and α_2 are calculated as

$$\frac{d\alpha_1}{dT} = \frac{\alpha_1(\beta_1 \Delta h_{cal1}(1-\alpha_1-\alpha_2) - 2\alpha_2\beta_2\Delta h_{cal2})}{RT^2(1+\alpha_2)} \qquad \text{(A17)}$$

$$\frac{d\alpha_2}{dT} = 2\alpha_2\left(\frac{\beta_2 \Delta h_{cal2}}{RT^2} + \frac{1}{\alpha_1}\frac{d\alpha_1}{dT}\right) \qquad \text{(A18)}$$

The total enthalpy for this system is

$$h_{tot} = h_N + \Delta h = h_N + \alpha_1 \Delta h_1 + \alpha_2(\Delta h_1 + \Delta h_2)$$

Then the total heat capacity (C_{tot}) can be obtained by differentiating the total enthalpy:

$$\begin{aligned} C_{tot} = \frac{dh}{dT} &= \frac{dh_N}{dT} + \frac{d\alpha_1}{dT}\Delta h_1 + \alpha_1\frac{d\Delta h_1}{dT} + \frac{d\alpha_2}{dT}(\Delta h_1 + \\ &\qquad \Delta h_2) + \alpha_2\left(\frac{d\Delta h_1}{dT} + \frac{d\Delta h_2}{dT}\right) \\ &= \Delta h_1\left(\frac{d\alpha_1}{dT} + \frac{d\alpha_2}{dT}\right) + \Delta h_2\frac{d\alpha_2}{dT} + (1-\alpha_1-\alpha_2)C_N + \\ &\qquad \alpha_1 C_D + \alpha_2 C_{D_2} \\ &= C_{ex} + C_{base} \end{aligned} \qquad \text{(A19)}$$

where

$$C_{ex} = \Delta h_1\left(\frac{d\alpha_1}{dT} + \frac{d\alpha_2}{dT}\right) + \Delta h_2\frac{d\alpha_2}{dT} \qquad \text{(A20)}$$

$$C_{base} = (1-\alpha_1-\alpha_2)C_N + \alpha_1 C_D + \alpha_2 C_{D_2} \qquad \text{(A21)}$$

Therefore, C_{tot} can be calculated by using eq A19. The experimental data were least-square-fitted utilizing the Marquardt method. The fitting parameters are t_{h1}, t_{h2}, Δh_{h1}, Δh_{h2}, β_1, and β_2. β_1 and β_2 can be fixed to the molecular weight. It is also possible to arbitrarily float any of the parameters, such as B_1 and B_2. This feature is especially useful for the case where eq A6 is not applicable for the intermediate state (C_{N_2}).

REFERENCES

Flory, P. J. (1956) *J. Am. Chem. Soc. 78*, 5222−5235.

Gitelson, G. I., Griko, Y. V., Kurochkin, A. V., Rogov, V. V., Kutyshenko, V. P., Kirpichnikov, M. P., & Privalov, P. L. (1991) *FEBS Lett. 289*, 201−204.

Griko, Y. V., Rogov, V. V., & Privalov, P. L. (1992) *Biochemistry 31*, 12701−12705.

Hiromi, K., Akasaka, K., Mitsui, Y., Tonomura, B., & Murao, S. (Eds.) (1985) *Protein Protease Inhibitor—The Case of Streptomyces Subtilisin Inhibitor (SSI)*, Elsevier, Amsterdam.

Hu, C.-Q., Kitamura, S., Tanaka, A., & Sturtevant, J. M. (1992a) *Biochemistry 31*, 1643−1647.

Hu, C.-Q., Sturtevant, J. M., Thomson, J. A., Erickson, R. E., & Pace, C. N. (1992b) *Biochemistry 31*, 4876−4882.

Izatt, R. M., & Christensen, J. J. (1970) Heat of Proton Ionization, pK, and Related Thermodynamic Quantities, in *Handbook of Biochemistry, Selected Data for Molecular Biology* (Sober, H. A., Ed.) pp J58−J173, CRC Press, Cleveland, OH.

Kauzmann, W. (1959) *Adv. Protein Chem. 14*, 1−63.

Kojima, S., Obata, S., Kumagai, I., & Miura, K. (1990) *Bio/Technology 8*, 449−452.

Ladbury, J. E., Hu, C.-Q., & Sturtevant, J. M. (1992) *Biochemistry 31*, 10699−10702.

Marquardt, D. W. (1963) *J. Soc. Ind. Appl. Math. 11*, 431−441.

Matsumura, M., & Matthews, B. W. (1991) *Methods Enzymol. 202*, 336−356.

Morinaga, Y., Franceschini, T., Inouye, S., & Inouye, M. (1984) *Bio/Technology 2*, 636−639.

Obata, S., Furukubo, S., Kumagai, I., Takahashi, H., & Miura, K. (1989) *J. Biochem. 105*, 372−376.

Pace, C. N., Grimsley, G. R., Thomson, J. A., & Barnett, B. J. (1988) *J. Biol. Chem. 263*, 11820−11825.

Privalov, P. L. (1979) *Adv. Protein Chem. 33*, 167−241.

Sauer, R. T., Hehir, K., Stearman, R. S., Weiss, M. A., Jeitler-Nilsson, A., Suchanek, E. G., & Pabo, C. O. (1986) *Biochemistry 25*, 5992−5998.

Sturtevant, J. M. (1987) *Annu. Rev. Phys. Chem. 38*, 463−488.

Sturtevant, J. M. (1994) *Curr. Opin. Struct. Biol. 4*, 69−78.

Takahashi, K., & Sturtevant, J. M. (1981) *Biochemistry 20*, 6185−6190.

Tamura, A., Kanaori, K., Kojima, S., Kumagai, I., Miura, K., & Akasaka, K. (1991a) *Biochemistry 30*, 5275−5286.

Tamura, A., Kimura, K., & Akasaka, K. (1991b) *Biochemistry 30*, 11313−11320.

Tamura, A., Kimura, K., Takahara, H., & Akasaka, K. (1991c) *Biochemistry 30*, 11307−11313.